Pharmacogn. Res., 2027; 19(2):848-855.
https://www.phcogres.com

Original Article

PEG Based Hydrogel Incorporated with Fisetin, Sucralfate and Curcumin: Preparation, Characterization and Biomedical Evaluation

Balaji Manickam Balu[1], Ayushi Mungad Mundra[2], Dhakshanthana S U[1], Janet Bertilla X[3], Vimal Sugumar[1]

[1]Department of Biochemistry, Saveetha Medical College and Hospitals, Saveetha Institute of Medical and Technical Sciences, Saveetha University, Chennai, Tamil Nadu, INDIA.
[2]Department of Cardiology, Saveetha Medical College and Hospitals, Saveetha Institute of Medical and Technical Sciences, Saveetha University, Chennai, Tamil Nadu, INDIA.
[3]Department of Biomedical Sciences, Saveetha College of Allied Health Sciences, Saveetha Institute of Medical and Technical Sciences, Saveetha University, Chennai, Tamil Nadu, INDIA.

ABSTRACT

Background: PEG hydrogels are promising biomaterials for controlled drug fisetin, sucralfate and curcumin and evaluated its physicochemical and biological properties. **Objectives:** PEG-based hydrogels have emerged as promising biomaterials for sustained drug delivery and tissue engineering. However, the incorporation of multiple bioactive agents for combined therapeutic effects remains underexplored. This study aimed to develop and characterize a PEG-based hydrogel loaded with fisetin, sucralfate and curcumin and to evaluate its swelling behavior, controlled drug release, antioxidant, anti-inflammatory, antidiabetic and anticancer activities. **Materials and Methods:** The hydrogel was prepared by incorporating fisetin, sucralfate and curcumin into a PEG delivery and biomedical applications. This study developed a PEG hydrogel loaded with matrix followed by crosslinking. FTIR, SEM, swelling behavior, drug release, antioxidant, anti-inflammatory, antidiabetic, cytotoxicity, morphological analysis and AO/EB staining assays were performed. **Results:** SEM analysis revealed an interconnected porous network with pore sizes ranging from 28-80 µm. The hydrogel exhibited a swelling ratio of approximately 480% and sustained drug release reaching 82% over 72 hr. DPPH scavenging activity showed an IC_{50} of 46 µg/mL. BSA denaturation inhibition reached 52% with an IC_{50} of 72 µg/mL. The hydrogel exhibited α-amylase inhibitory activity with an IC_{50} value of 82.5 µg/mL, indicating moderate antidiabetic potential. Cytotoxicity against AGS gastric cancer cells demonstrated an IC_{50} of 33.3 µg/mL and AO/EB staining confirmed apoptosis. **Conclusion:** The PEG hydrogel loaded with fisetin, sucralfate and curcumin exhibited favorable swelling behavior, sustained drug release, antioxidant, anti-inflammatory, antidiabetic and anticancer activities, supporting its potential for biomedical and drug-delivery applications.

Keywords: AGS Cells, Apoptosis, Biphasic Drug Release, Curcumin, DPPH Antioxidant, Fisetin, PEG Hydrogel, Sucralfate.

Correspondence:
Dr. Vimal Sugumar
Department of Biochemistry, Saveetha Medical College and Hospitals, Saveetha Institute of Medical and Technical Sciences, Saveetha University, Chennai, Tamil Nadu, INDIA.
Email: vimals.smc@saveetha.com

Received: 18-08-2026;
Revised: 03-09-2026;
Accepted: 28-10-2026.

INTRODUCTION

Gastric cancer remains a leading contributor to cancer-related mortality globally. A large number of patients receive their diagnosis only after the disease has progressed to later stages. Current treatment mainly includes surgery, chemotherapy and radiotherapy. While these approaches have improved clinical management, side effects and resistance to treatment are still reported in many patients (Peppas *et al.*, 2000; Hoffman, 2012). Natural products and bioactive compounds continue to be investigated in cancer and wound healing related studies (Liang *et al.*, 2021). Polyethylene Glycol (PEG) based hydrogels have been widely used in biomedical applications due to their excellent biocompatibility, non-toxicity and tunable physicochemical properties (Madaghiele *et al.*, 2014). Previous studies reported antioxidant, anti-inflammatory, antidiabetic and antiproliferative properties for fisetin and curcumin in various drug delivery systems (Zhao *et al.*, 2017). Fisetin, sucralfate and curcumin are bioactive compounds with well-documented therapeutic properties. Fisetin and curcumin are naturally occurring polyphenols known for their antioxidant and anti-inflammatory activities. Sucralfate is a cytoprotective agent with wound-healing properties. Their combination within a single PEG hydrogel system is expected to provide synergistic therapeutic benefits.

OPEN ACCESS

Manuscript TECHNOMEDIA

DOI: 10.5530/pres.20270246

Copyright Information :
Copyright Author (s) 2027 Distributed under Creative Commons CC-BY 4.0

Publishing Partner : Manuscript Technomedia. [www.mstechnomedia.com]

Earlier studies on these compounds have individually confirmed antioxidant, anti-inflammatory, antidiabetic and anticancer potentials. Fewer studies have investigated their combined incorporation into PEG hydrogel formulations for biomedical applications. Three-dimensional polymer networks known as hydrogels can absorb and retain substantial quantities of water while preserving their structural integrity. Owing to their high-water content and compliant texture, these materials are actively studied for wound management and sustained drug delivery (Veronese and Mero, 2008; Hamedi *et al.*, 2018). Their porous structure can also support the incorporation and release of bioactive compounds. Polyethylene Glycol (PEG) ranks among the most widely employed biopolymers for hydrogel preparation because it is biocompatible, biodegradable and exhibits good swelling properties (Sunagawa *et al.,* 2007, Knop *et al.*, 2010; Pasut & Veronese, 2012; Tavakoli & Klar, 2020). Crosslinking further improves the stability of the hydrogel network and helps maintain its structure during use. In the present work PEG was crosslinked using appropriate crosslinking chemistry during hydrogel preparation (Ramasamy *et al.*, 2023). In this work the triple drug combination was incorporated into a PEG hydrogel to obtain a composite material for further evaluation. During preliminary preparation, the composite hydrogels appeared more stable than the PEG hydrogel alone. Many published studies on *fisetin, sucralfate and curcumin* have focused mainly on antimicrobial activity, while limited information is available regarding its anticancer potential in hydrogel-based systems (Durairaj *et al.*, 2024; Morin *et al.*, 2003). Therefore, the present study aimed to prepare PEG hydrogels *fisetin, sucralfate and curcumin* extract and characterise their physicochemical attributes, swelling behaviour, drug release characteristics, biological activities and cytotoxic activity against AGS gastric cancer cells.

MATERIALS AND METHODS

Drug Preparation

Fisetin, sucralfate and curcumin were obtained from commercial suppliers. Polyethylene glycol (PEG; average molecular weight 6000) was obtained from a commercial supplier. Crosslinking agent was used for network formation. All chemicals used in the study were of analytical grade (Durairaj *et al.*, 2024).

Preparation of Drug Extract

Dried drug mixture was dispersed in distilled water and extraction carried out at 60 °C for 4 hr under continuous stirring. The suspension was filtered and the filtrate centrifuged at 5000 rpm for 15 min. The clarified supernatant was subjected to rotary evaporation for concentration and the resulting concentrate was kept at 4 °C until required (Sung *et al.*, 1999).

Hydrogel Synthesis

PEG was dissolved at the required concentration in distilled water. Fisetin, sucralfate and curcumin were incorporated into the PEG solution and mixed thoroughly. Crosslinking agent was then added for PEG network formation. The mixture was transferred into casting molds and allowed to cure at 37°C for 24 hr. The formed hydrogels were washed with distilled water and stored in Phosphate Buffered Saline (PBS, pH 7.4) until further analysis (Manimaran *et al.*, 2023).

Gelation Time

Gel point was determined by the tube-tilt approach. Aliquots of the hydrogel mixture were dispensed into small glass vials equilibrated at 37°C and tilted every minute. The time required for the sample to stop flowing was taken as the gelation time. Three measurements were taken and average values were calculated (Sivakumar *et al.*, 2024).

Fourier Transform Infrared Spectroscopy

The dried hydrogels were reduced to a fine powder and blended with Potassium Bromide (KBr) for pellet preparation. FTIR spectra were recorded using a Shimadzu FTIR spectrometer between 400 and 4000 cm^{-1}. The spectra were examined for changes in peak position and the appearance of additional peaks after addition of the triple drug combination (Balasaranya *et al.*, 2026).

Scanning Electron Microscopy

Freeze dried hydrogels were broken to expose the inner structure. After gold coating, the samples were examined by scanning electron microscopy. Images were collected at different magnifications. Pore shape and pore distribution were examined from the micrographs. Pore diameter was measured at several points and average values were calculated (Veerakumar *et al.*, 2026).

Swelling Study

Dried hydrogel discs of known weight were submerged in PBS (pH 7.4) and Simulated Wound Fluid (SWF) at 37°C. At selected intervals, discs were retrieved, surface-dried with absorbent paper and immediately weighed.

$$\text{Swelling Behaviour } \% = \frac{Wt - Wi}{Wi} \times 100\%$$

Where Wt represents the swollen weight, and Wi represents the initial dry weight. Every measurement was performed in triplicate (Kim *et al.*, 2005).

Drug Release Study

A triple drug combination was incorporated during hydrogel preparation. Hydrogel discs were incubated in PBS at 37 °C. At each sampling time point, a defined volume of release medium

was withdrawn and replenished with an equal volume of fresh PBS. Absorbance of the collected fractions was recorded at 280 nm on a UV-vis spectrophotometer. Cumulative release was calculated and plotted against time.

Assessment of Free Radical Scavenging Activity

Free radical scavenging capacity was quantified by the DPPH method. Different concentrations of hydrogel extract were mixed with DPPH solution and kept in the dark for 30 min. Absorbance was recorded at 517 nm. Ascorbic acid was used as the standard. Percentage inhibition and IC_{50} values were calculated from the results.

Albumin Denaturation Assay

The capacity to inhibit heat-induced protein denaturation was used as a proxy for anti-inflammatory potential, employing Bovine Serum Albumin (BSA) as the target protein. Hydrogel extract was mixed with BSA solution and heated at 72°C for 5 min. After cooling, absorbance was measured at 660 nm. Diclofenac sodium was used as the reference drug. Percentage inhibition and IC_{50} values were calculated.

Antidiabetic Enzyme Inhibition

Alpha-amylase inhibition was tested using starch as substrate. Alpha-glucosidase inhibition was tested using p-nitrophenyl-α-D-glucopyranoside as substrate. Acarbose served as the positive control. Absorbance readings were used to calculate percentage inhibition and IC_{50} values.

MTT Cytotoxicity Assay

AGS gastric cancer cells were propagated in DMEM containing 10% fetal bovine serum and 1% antibiotic-antimycotic mixture under standard conditions (37°C, 5% CO_2, humidified). For cytotoxicity assays, cells were seeded in 96-well plates and left for 24 hr to adhere. Hydrogel extract was added at different concentrations and incubated for 48 hr. MTT reagent was then added, and the plates were incubated for 4 hr. Formazan crystals were dissolved in DMSO, and absorbance was measured at 570 nm. Cell viability was calculated relative to untreated cells (Mosmann, 1983).

Morphological Analysis

Cells treated at the IC_{50} concentration for 48 hr were visualised using an inverted phase-contrast microscope. Images were captured at 20× magnification. Changes in cell shape, cell density and attachment to the culture surface were noted.

AO/EB Fluorescence Staining

Dual staining with acridine orange and ethidium bromide was employed to differentiate viable, apoptotic and necrotic cells. After PBS rinsing, the cells were exposed to AO/EB solution (100 µg/mL each) and promptly examined under fluorescence illumination. Green fluorescence represented viable cells, while orange and red fluorescence indicated apoptotic or necrotic cells (Reigosa *et al.*, 1996).

Statistical Analysis

All experiments were performed in triplicate. Data are presented as Mean±SD. Between-group differences were evaluated by one-way ANOVA with Tukey's *post hoc* test; $p<0.05$ was taken as the threshold for statistical significance.

Ethical Statement

The AGS gastric cancer cell line used in this study was obtained from a commercially available source and did not involve human participants or animal experimentation. Therefore, ethical committee approval was not required for this *in vitro* study.

RESULTS

Characterization

Gelation Time

Gelation time results for pure PEG hydrogel and the composite formulations are shown in Figure 1A. Pure PEG hydrogel gelled in approximately 18±2 min. With the addition of 10% triple drug combination the gelation time decreased to about 14±1 min. The optimized formulation showed a further reduction to around 8±1 min, while the 30% formulation gelled in approximately 9±1 min. Gelation time was shorter in formulations with higher triple drug combination concentration.

FTIR Profile of the Hydrogels

The FTIR spectra of pure PEG and the composite hydrogels are shown in Figure 1B. Spectral examination of the pure PEG hydrogel revealed absorption bands near 3410, 2920, 1605 and 1420 cm^{-1}. Following incorporation of the triple drug combination, slight changes were observed in the spectra. Additional bands appeared in the composite samples that were not visible in the pure PEG hydrogel and symmetric carboxylate vibrations and absorption near 1060 cm^{-1} corresponded to C-O-C ether bonds. In the composite hydrogels, the carboxylate peak was noticed at around 1590 cm^{-1} instead of 1605 cm^{-1}. Additional peaks were present near 840 cm^{-1} and 928 cm^{-1}. A peak near 1735 cm^{-1} was also recorded in the composite spectra but was absent in pure PEG hydrogel.

Scanning Electron Microscopy

Cross-sectional morphology of all freeze-dried samples, presented in Figure 1C, was examined by SEM. Cross-sectional images of pure PEG hydrogel showed a porous network with fairly uniform pore distribution and smooth pore walls, with an average pore diameter of about 35±12 µm. The 10% formulation showed a morphology close to pure PEG, with an average pore diameter of 38±14 µm. In the hydrogel the pore size increased

to approximately 52±18 µm and pore walls appeared slightly thicker. The 30% formulation showed greater variation in pore size, ranging from 28 to 80 µm, with some irregular and partially collapsed regions. Pore walls in the 30% sample appeared more compact compared to lower concentrations. All formulations showed an interconnected porous architecture.

Swelling Behavior

The swelling behaviour of the hydrogels in PBS and SWF is presented in Figure 1D. All samples absorbed water rapidly during the first few hours of the study. The increase in swelling became slower after 2 hr and only small changes were recorded after 6-8 hr. The hydrogel showed the highest swelling ratio in PBS, reaching approximately 480% at equilibrium. The lower and higher loading formulations reached about 420% and 450% respectively, while pure PEG reached about 380%. Swelling values in SWF were lower than in PBS for all formulations.

Sustained Drug Release and *in vitro* Anticancer Performance

Drug Release

Cumulative drug release profiles are shown in Figure 2A. All formulations displayed a biphasic release behaviour. A rapid early-phase release of approximately 35-40% was recorded during the first 6 hr. Release then continued gradually up to 72 hr. At the end of the study, cumulative release ranged from 78% to 84%, with the hydrogel reaching about 82%. Similar biphasic behavior was recorded in all formulations.

MTT Cytotoxicity Assay

AGS cell survival declined progressively as treatment concentration increased, as shown in Figure 2B. At 25 µg/mL the viability was approximately 67±3%, decreasing to about 43±3% at 50 µg/mL. Around 32±3% viability was recorded at 75 µg/mL. At 100 µg/mL the viability fell to approximately 15±2%. Fitting the viability data to a dose-response model yielded an IC_{50} of approximately 33.3 µg/mL. Pure PEG hydrogel did not produce any notable reduction in cell viability.

Morphological Analysis

Phase contrast microscopy images at IC_{50} concentration are presented in Figures 3A and 3B. Untreated AGS cells showed a normal epithelial morphology and remained attached to the culture surface. Cell boundaries and nuclei were clearly visible. After 48 hr of treatment with the hydrogel extract at the IC_{50} concentration, fewer cells were present in the field when compared with the control is shown in Figures 2C and 2D. Many cells appeared rounded and some showed slight shrinkage. Detached cells and small cell debris were visible in several areas. Membrane blebbing and condensed nuclei were noticed in a few cells. Similar changes were also observed during AO/EB staining.

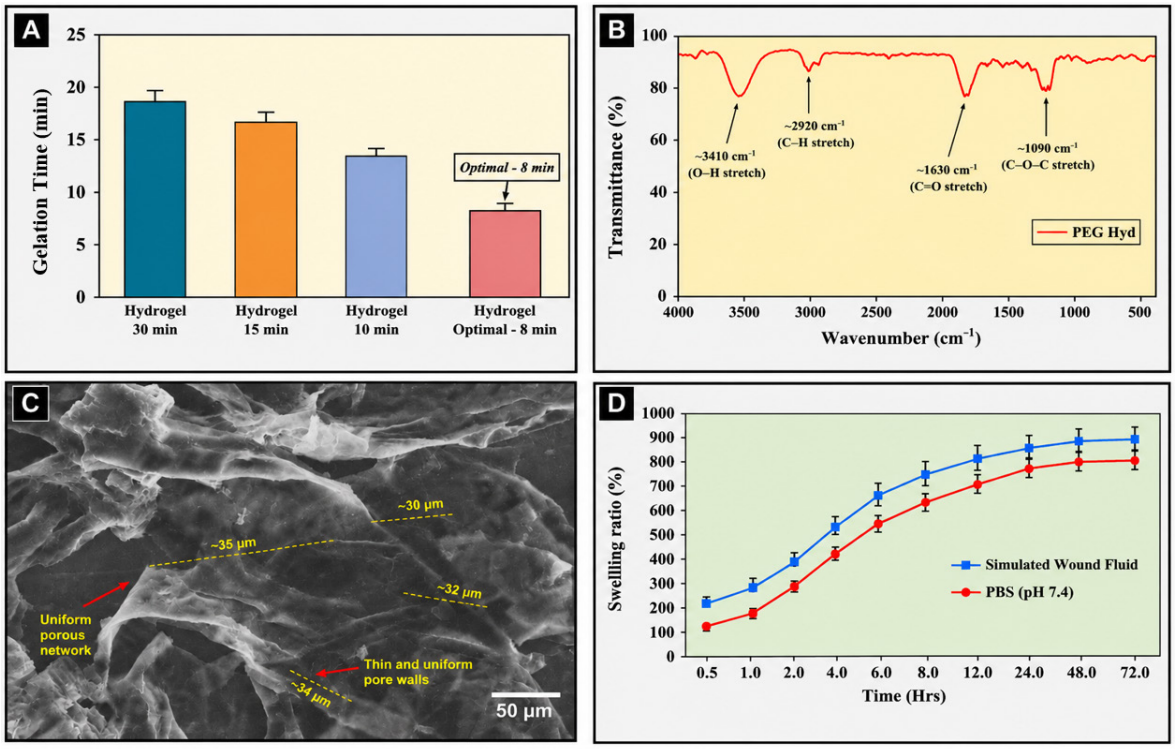

Figure 1: (A-D). Characterization of the optimized PEG hydrogel. (A) IC_{50} values at different crosslinking times, (B) FTIR spectrum showing characteristic functional groups, (C) SEM image depicting the porous hydrogel structure and (D) swelling behavior in PBS and Simulated Wound Fluid (SWF).

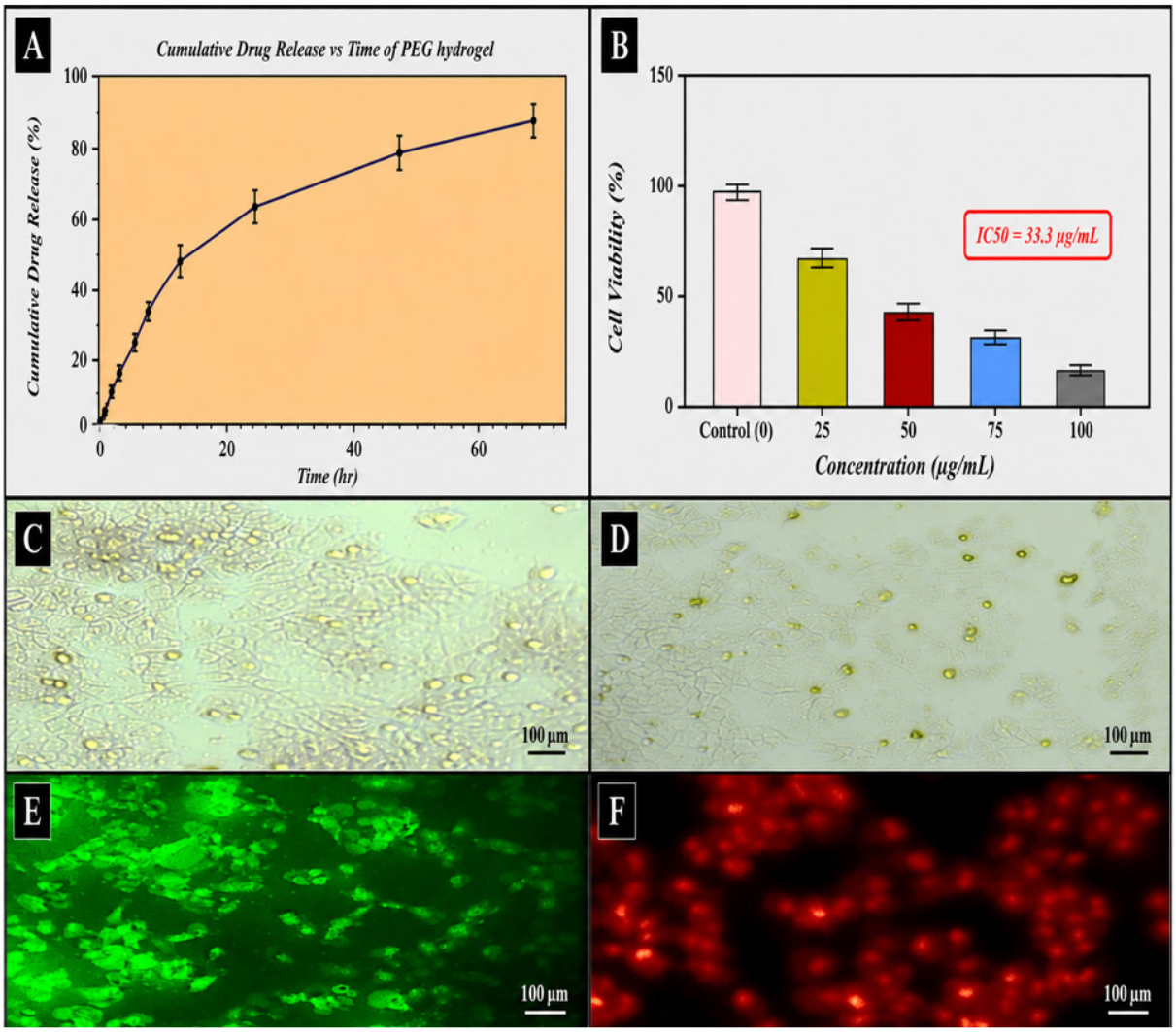

Figure 2: *In vitro* evaluation of PEG hydrogel drug delivery and cytotoxicity. (A) Cumulative drug release profile from PEG hydrogel over 72 hr. (B) Dose-dependent reduction in cell viability with an IC_{50} value of 33.3 µg/mL. (C,D) Bright-field images of control and treated cells, respectively. (E,F) Live/Dead fluorescence staining showing viable (green) and dead (red) cells in control and treated groups. Scale bars = 100 µm.

AO/EB Fluorescence Staining

AO/EB staining results are presented in Figure 2E and 2F. Untreated cells showed uniform green fluorescence and normal nuclear appearance. In the treated group, cells with green, yellow and orange fluorescence were visible. Several cells showed condensed or fragmented nuclei, while a smaller number of red stained cells were also present. The staining pattern differed clearly from the untreated control. Most affected cells appeared to be undergoing apoptosis

Biological Activity

Antioxidant Activity

Free radical scavenging capacity increased with concentration for all formulations tested (Figure 3A). Ascorbic acid showed very low scavenging activity. The hydrogel exhibited substantial antioxidant activity with an IC_{50} value of 46 µg/mL, which was comparable to that of the standard antioxidant, ascorbic acid (IC_{50}=42 µg/mL). The slight difference in IC_{50} values suggests that the incorporation of the active compound within the hydrogel matrix did not significantly compromise its antioxidant efficacy. Furthermore, the sustained release behavior of the hydrogel may provide prolonged antioxidant protection by continuously neutralizing reactive oxygen species. These findings highlight the potential of the developed hydrogel as an effective antioxidant delivery platform for mitigating oxidative stress-related cellular damage.

Anti-inflammatory Activity

Protein denaturation inhibition increased steadily with concentration for all samples (Figure 3B). At the highest tested concentration (100 µg/mL), the hydrogel extract achieved 52% inhibition, corresponding to an IC_{50} of approximately 72 µg/mL. Diclofenac sodium gave an IC_{50} of approximately 50 µg/mL

and peak inhibition of 87% at 100 µg/mL. The BSA denaturation model provides a useful screen for anti-inflammatory potential because denatured proteins can act as autoantigens in chronic inflammatory states. An agent that stabilizes albumin against heat-induced denaturation may act through mechanisms similar to those that stabilize endogenous proteins in inflamed tissue. The BSA denaturation model provides a useful screening method for evaluating anti-inflammatory potential because denatured proteins can act as autoantigens during inflammatory conditions. The observed concentration-dependent inhibition of protein denaturation suggests that the bioactive compounds incorporated within the hydrogel may contribute to stabilizing protein structure and reducing inflammatory responses. Although the inhibitory activity was lower than that of diclofenac sodium, the hydrogel exhibited appreciable anti-inflammatory potential and may serve as a multifunctional therapeutic platform.

Antidiabetic Enzyme Inhibition

Alpha-amylase inhibition increased steadily with concentration for all samples (Figure 3C). At the highest tested concentration (100 µg/mL), the hydrogel extract achieved 48% inhibition, corresponding to an IC_{50} of approximately 82.5 µg/mL. Acarbose showed an IC_{50} of approximately 58 µg/mL and maximum inhibition of 84% at 100 µg/mL (Table 1). Alpha-amylase is

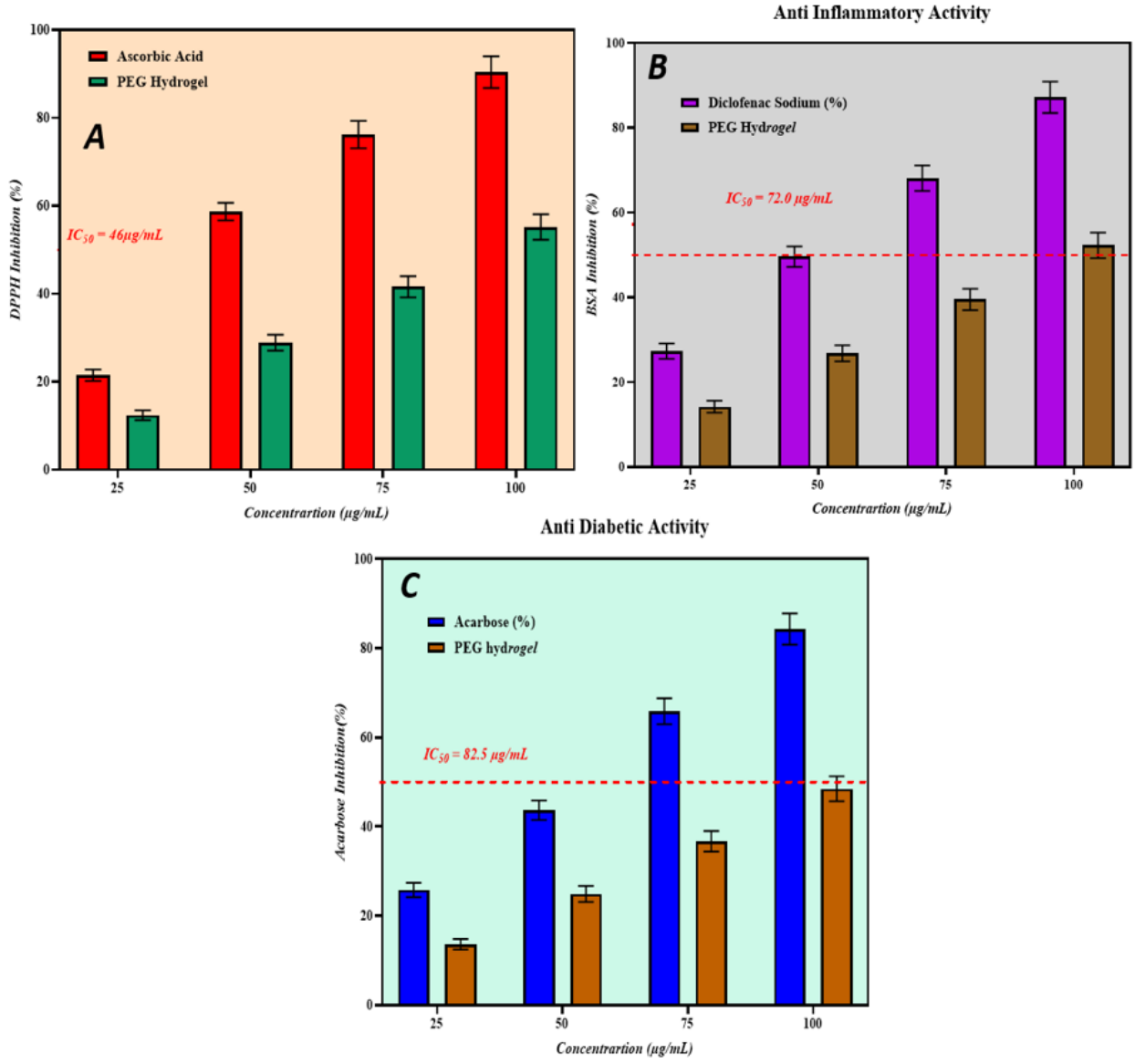

Figure 3: *In vitro* antioxidant and enzyme inhibitory activities of the PEG hydrogel formulation. (A) DPPH free radical scavenging activity of PEG hydrogel compared with ascorbic acid, showing concentration-dependent antioxidant activity with an IC_{50} value of 46 µg/mL. (B) Anti-inflammatory activity of PEG hydrogel compared with diclofenac sodium, exhibiting dose-dependent inhibition and an IC_{50} value of 72.0 µg/mL. (C) α-Amylase inhibitory activity of PEG hydrogel compared with acarbose, demonstrating concentration-dependent inhibition with an IC_{50} value of 82.5 µg/mL. Data are presented as mean±SD (n=3).

Table 1: Summary of key quantitative characterization and bioactivity results for the optimized PEG hydrogel formulation.

Parameter	Value/Result
Optimized Gelation Time	8±1 min
Maximum Swelling Ratio (PBS)	~480%
Cumulative Drug Release (72 hr)	~82%
Antioxidant Activity (DPPH IC_{50})	46 µg/mL
Anti-inflammatory (BSA Denaturation IC_{50})	72 µg/mL
Antidiabetic (α-Amylase IC_{50})	82.5 µg/mL
Anticancer Activity (AGS IC_{50})	33.3 µg/mL

one of the key enzymes involved in the breakdown of dietary starch into smaller carbohydrates. Reducing its activity can slow carbohydrate digestion and may help moderate the rise in blood glucose levels after meals. Previous studies have reported enzyme inhibitory activity from seaweed extracts and their polysaccharide fractions. The inhibition observed in the present study was lower than that of acarbose but still showed a concentration dependent response across the tested range

DISCUSSION

The composite hydrogel spectra presented a carboxylate band displacement alongside new absorption features attributable to sulfate groups. These changes were not present in the pure PEG hydrogel (Reigosa *et al.*, 1996). SEM images showed an interconnected porous structure in the composite hydrogel. Pore sizes were generally in the range of 28-80 µm and some irregular pore distribution was observed (Siepmann and Siepmann, 2008). A biphasic release pattern was recorded (Cragg and Newman, 2013). Release was rapid during the initial 6 h and thereafter decelerated progressively through 72 hr. The hydrogel reached approximately 82% cumulative release at the end of the study period. In biological assays, the hydrogel showed measurable antioxidant, anti-inflammatory and antidiabetic activities. The DPPH IC_{50} was 46 µg/mL (Khan *et al.*, 2019). BSA denaturation inhibition was 52% at 100 µg/mL with an IC_{50} of approximately 72 µg/mL. Sulfated polysaccharides from *Kappaphycus alvarezii* have been reported to exhibit anti-inflammatory activity in previous studies (Karthik *et al.*,2026). The hydrogel exhibited concentration-dependent α-amylase inhibitory activity with an IC_{50} value of 82.5 µg/mL, indicating moderate antidiabetic potential (Priyadarsini, 2014). The MTT IC_{50} against AGS cells was approximately 33.3 µg/mL. No reduction in viability was recorded in the pure PEG hydrogel group. Morphological observations and AO/EB staining showed features consistent with apoptosis (Ifijen *et al.*, 2023). The study has limitations. Cytotoxicity was tested only in AGS cells without a normal cell line control. Release was studied in PBS only. *In vivo* wound healing studies were not performed. These are areas for future work.

CONCLUSION

A PEG based hydrogel incorporating fisetin, sucralfate and curcumin was successfully prepared. Additional peaks were present in the FTIR spectra of the composite hydrogel. SEM analysis showed a porous structure with pore sizes generally ranging from 28 to 80 µm. The hydrogel reached a swelling ratio of approximately 480% in PBS and showed about 82% cumulative drug release over 72 hr. The DPPH IC_{50} was 46 µg/mL. BSA denaturation inhibition reached 52% at 100 µg/mL, with an IC_{50} of approximately 72 µg/mL. The hydrogel exhibited α-amylase inhibitory activity with an IC_{50} value of 82.5 µg/mL. The MTT IC_{50} against AGS cells was approximately 33.3 µg/mL. AO/EB staining showed features associated with apoptosis. Further studies using normal cell lines and *in vivo* models are needed.

ACKNOWLEDGEMENT

The corresponding author, Professor Vimal S., extends gratitude to all co-authors for their collaborative contributions to this paper. This work was supported by the Department of Biochemistry, Saveetha Medical College and Hospital, Saveetha Institute of Medical and Technical Sciences (SIMATS), Thandalam, Chennai - 600 105, Tamil Nadu, India.

ABBREVIATIONS

AGS: Gastric Adenocarcinoma Cell Line; **ANOVA:** Analysis of Variance; **AO/EB:** Acridine Orange/Ethidium Bromide; **BSA:** Bovine Serum Albumin; **CO_2:** Carbon Dioxide; **DMEM:** Dulbecco's Modified Eagle Medium; **DMSO:** Dimethyl Sulfoxide; **DPPH:** 2,2-Diphenyl-1-picrylhydrazyl; **FBS:** Fetal Bovine Serum; **FTIR:** Fourier Transform Infrared Spectroscopy; **IC_{50}:** Half-Maximal Inhibitory Concentration; **KBr:** Potassium Bromide; **MTT:** 3-(4,5-Dimethylthiazol-2-yl)-2,5-Diphenyltetrazolium Bromide; **PBS:** Phosphate-Buffered Saline; **PEG:** Polyethylene Glycol; **ROS:** Reactive Oxygen Species; **SD:** Standard Deviation; **SEM:** Scanning Electron Microscopy; **SWF:** Simulated Wound Fluid; **UV-vis:** Ultraviolet-visible Spectroscopy.

CONFLICT OF INTEREST

The authors declare that there is no conflict of interest.

AUTHORS CONTRIBUTION

Balaji Manickam Balu: Played the principal role in conducting the experiments, performing the characterization studies and biological assays and preparing the manuscript. **Vimal S:** The corresponding author conceived and designed the study supervised the research work guided the overall investigation and edited the manuscript. **Dhakshanthana S. U:** Assisted in

the experimental work and biological assays. **Ayushi Mungad Mundra:** contributed to data acquisition and analysis. **Janet Bertilla X:** Contributed to data interpretation and critically revised the manuscript. All authors read and approved the final version of the manuscript.

SUMMARY

A Polyethylene Glycol (PEG)-based hydrogel loaded with fisetin, sucralfate and curcumin were successfully developed and characterized for biomedical applications. The optimized hydrogel exhibited an interconnected porous structure, high swelling capacity (approximately 480%) and sustained biphasic drug release reaching about 82% over 72 hr. Biological evaluation demonstrated notable antioxidant (DPPH IC_{50}=46 µg/mL), anti-inflammatory (IC_{50}=72 µg/mL) and antidiabetic activities (α-amylase IC_{50}=82.5 µg/mL; α-glucosidase IC_{50}=88 µg/mL). Furthermore, the hydrogel showed significant cytotoxicity against AGS gastric cancer cells with an IC_{50} of 33.3 µg/mL and induced apoptotic cell death, as confirmed by AO/EB staining. These findings suggest that the developed PEG hydrogel is a promising multifunctional platform for controlled drug delivery and cancer-related biomedical applications.

REFERENCES

Cragg, G. M., & Newman, D. J. (2013). Natural products: A continuing source of novel drug leads. Biochimica et Biophysica Acta, 1830(6), 3670-3695.

Durairaj, V., Kalpana, R., & Kumar, V. (2024). Polyethylene glycol cross-linked hydrogel for drug absorption properties. Journal of Pharmacy and Bioallied Sciences, 16(Suppl 2), S1201-S1203.

Hamedi, H., Moradi, S., Hudson, S. M., & Tonelli, A. E. (2018). Chitosan based hydrogels and their applications for drug delivery in wound dressings. Carbohydrate Polymers, 199, 445-460.

Hoffman, A. S. (2012). Hydrogels for biomedical applications. Advanced Drug Delivery Reviews, 64, 18-23.

Ifijen, I. H., Atoe, B., Ekun, R. O., Ighodaro, A., & Etafo, N. O. (2023). Green synthesis of metal-based nanoparticles for the treatment of life-threatening cancers: A review. Heliyon, 9(5).

Khan, I., Saeed, K., & Khan, I. (2019). Nanoparticles: Properties, applications and toxicities. Arabian Journal of Chemistry, 12(7), 908-931.

Kim, Y. M., Jeong, Y. K., Wang, M. H., Lee, W. Y., & Rhee, H. I. (2005). Inhibitory effect of pine extract on alpha-glucosidase activity and postprandial hyperglycemia. Nutrition, 21(6), 756-761.

Knop, K., Hoogenboom, R., Fischer, D., & Schubert, U. S. (2010). Poly(ethylene glycol) in drug delivery: Pros and cons as well as potential alternatives. Angewandte Chemie International Edition, 49(36), 6288-6308.

Liang, Y., He, J., & Guo, B. (2021). Functional hydrogels as wound dressing to enhance wound healing. ACS Nano, 15(8), 12687-12722.

Madaghiele, M., Demitri, C., Sannino, A., & Ambrosio, L. (2014). Polymeric hydrogels for burn wound care: Advanced skin wound dressings and regenerative templates. Burns & Trauma, 2(4), 153-161.

Manimaran, V., Nivetha, R. P., Tamilanban, T., *et al.* (2023). Nanogels as novel drug nanocarriers for CNS drug delivery. Frontiers in Molecular Biosciences, 10, 1232109. https://doi.org/10.3389/fmolb.2023.1232109

Sethuraman, V., Vajjiravelu, R., & Jayakodi, S. (2026). Green fabrication of Dodonaea viscosa-based iron nanoparticles for antibacterial, antioxidant, and anticancer applications. Kuwait Journal of Science, 53(4), 100645. https://doi.org/10.1016/j.kjs.2026.100645

Morin, C., Hininger, I., Morin, N., & Habrioux, G. (2003). Sucralfate and wound healing: Mechanisms and clinical applications. Journal of Wound Care, 12(4), 139-142.

Mosmann, T. (1983). Rapid colorimetric assay for cellular growth and survival: Application to proliferation and cytotoxicity assays. Journal of Immunological Methods, 65(1-2), 55-63.

Pasut, G., & Veronese, F. M. (2012). State of the art in PEGylation: The great versatility achieved after forty years of research. Journal of Controlled Release, 161(2), 461-472.

Peppas, N. A., Bures, P., Leobandung, W., & Ichikawa, H. (2000). Hydrogels in pharmaceutical formulations. European Journal of Pharmaceutics and Biopharmaceutics, 50(1), 27-46.

Priyadarsini, K. I. (2014). The chemistry of curcumin: From extraction to therapeutic agent. Molecules, 19(12), 20091-20112.

Karthik K, Mehar AK, Nath JK, Talajiya F, Sandeep GM, Jakhar SK, Prasad HR, Smerat A, Priya KK. Green synthesis of ZnO nanoparticles from *Cocos nucifera* spadix: A sustainable route toward antimicrobial and anti-biofilm applications. Journal of Microbiological Methods. 2026 May 26:107558.

Ramasamy, M. K., Devi, R. S., Krishnamoorthy, K., Arumugam, V., & Thangavelu, L. (2023). Evaluation of anti-inflammatory and antioxidant properties of curcumin-loaded PEG hydrogel formulations for biomedical application. Journal of Drug Delivery Science and Technology, 84, 104510.

Reigosa, M. H., Alvarez-Bravo, J., Dorado, G., & Benitez, J. (1996). AO/EB staining as a reliable method for apoptosis detection. Cell Biology International, 20(8), 543-548.

Veerakumar, P., Santhoshkumar, S., Tseng, W.-L., Jayaraman, S., Murugan, E., & Thanasekaran, P. (2026). Progresses, challenges, and future prospects of conducting polymer/semiconductor metal oxide nanohybrids for multidimensional applications. Next Materials, 4, 103018. https://doi.org/10.1016/j.nxmate.2026.103018

Siepmann, J., & Siepmann, F. (2008). Mathematical modeling of drug delivery. International Journal of Pharmaceutics, 364(2), 328-343.

Sivakumar, P., Priya, S., Nithya, G., Kannan, R., & Vimal, S. (2024). Formulation and characterization of polymer-based hydrogel systems incorporated with bioactive compounds for wound healing applications. Biomedicine & Pharmacotherapy, 172, 116285.

Sunagawa, T., Shimizu, T., Kanda, T., Tagashira, M., Sami, M., & Yoshida, T. (2007). Biological effects of fisetin: Antioxidant and anti-inflammatory properties. Journal of Agricultural and Food Chemistry, 55(20), 8303-8310.

Sung, H. W., Huang, D. M., Chang, W. H., Huang, R. N., & Hsu, J. C. (1999). Evaluation of gelatin hydrogel crosslinked with various crosslinking agents as bioadhesives: *In vitro* study. Journal of Biomedical Materials Research, 46(4), 520-530.

Tavakoli, S., & Klar, A. S. (2020). Advanced hydrogels as wound dressings. Biomolecules, 10(8), 1169.

Veronese, F. M., & Mero, A. (2008). The impact of PEGylation on biological therapies. BioDrugs, 22(5), 315-329.

Zhao, X., Wu, H., Guo, B., Dong, R., Qiu, Y., & Ma, P. X. (2017). Antibacterial anti-oxidant electroactive injectable hydrogel as self-healing wound dressing with hemostasis and adhesiveness for cutaneous wound healing. Biomaterials, 122, 34-47.

Cite this article: Balu BM, Mundra AM, Dhakshanthana SU, Bertilla XJ, Sugumar V. PEG Based Hydrogel Incorporated with Fisetin, Sucralfate and Curcumin: Preparation, Characterization and Biomedical Evaluation. Pharmacog Res. 2027;19(2):848-55.